phys. stat. sol. (b) 68, 405 (1975)

Subject classification: 13.1; 22.1; 22.1.1; 22.1.2; 22.2.1; 22.4.2

Department of Physics, University of California, and
Inorganic Materials Research Division,
Lawrence Berkeley Laboratory, Berkeley, California

Tight-Binding Calculations of the Valence Bands of Diamond and Zincblende Crystals

By

D. J. CHADI and M. L. COHEN

Using the tight-binding method, the valence band structures and densities of states for C, Si, Ge, GaAs, and ZnSe are calculated. Very good agreement is obtained with other calculations when all nearest- and one second-nearest-neighbor interactions are included. The effects of the various interactions on the density of states are discussed.

Mit der „tight-binding"-Methode werden die Valenzbandstrukturen und Zustandsdichten für C, Si, Ge, GaAs und ZnSe berechnet. Sehr gute Übereinstimmung mit anderen Rechnungen wird erreicht, wenn alle Wechselwirkungen mit nächsten und nur eine Wechselwirkung mit zweitnächsten Nachbarn berücksichtigt werden. Die Einflüsse verschiedener Wechselwirkungen auf die Zustandsdichte werden diskutiert,

1. Introduction

The tight-binding approach to the problem of the electronic energy levels in solids is intuitively very appealing. The method provides a real space picture of the electronic interactions which give rise to the particular features of the energy band structure, density of states, etc. This is extremely useful in studies of how these features change when the electronic configuration is altered. The tight-binding method is most practical when only a few types of electronic interactions are dominant. In such a case an adequate description of the system of interest can be obtained by specifying a small number of interaction parameters. In this way a qualitative description of the valence bands can be obtained [1 to 8] for materials in the diamond, zincblende, and other structures.

In this paper we show that a tight-binding method using a few interaction parameters gives accurate results for the valence bands of the diamond and zincblende crystals C, Si, Ge, GaAs, and ZnSe. The tight-binding method we use is equivalent to that of Slater and Koster [6]. It can also be regarded as a more complete version of the Weaire and Thorpe [2] model in which interactions between more distant directed orbitals are included. It is necessary to include these extra interactions for a more complete description of the valence bands. In Section 2 we give a brief review of the method and consider the effects of the various interactions on the density of states. We show that the inclusion of all the possible nearest-neighbor interactions[1]) between s- and p-tight-binding states is not sufficient to broaden the "p-like" bands along all symmetry directions. The resulting error in the energies is about 1 eV and occurs mostly for

[1]) By nearest-neighbor interactions we mean interactions of orbitals on nearest-neighbor atoms.

states near the surface of the Brillouin zone. With the inclusion of only one second-nearest-neighbor interaction, the accuracy is greatly improved and the resulting valence band structures and densities of states exhibit all the structures obtained in other calculations.

The band structures, densities of states, and interaction parameters for C, Si, Ge, GaAs, and ZnSe are discussed in Section 3. The dependence of the energy levels, along several symmetry directions and at some symmetry points, on the interaction parameters are also given in Section 3. These expressions are useful for obtaining information about the interaction parameters.

2. Tight-Binding Method

In diamond and zincblende crystals, every atom is tetrahedrally coordinated and there are two atoms in the primitive cell. For each tight-binding basis function centered on these atoms, two Bloch functions can be constructed. For example, for a tight-binding basis function $b(\boldsymbol{r})$ we have the two Bloch functions

$$\psi_0(\boldsymbol{k}, \boldsymbol{r}) = \frac{1}{\sqrt{N}} \sum_{\boldsymbol{R}} e^{i\boldsymbol{k}\cdot\boldsymbol{R}}\, b_0(\boldsymbol{r} - \boldsymbol{R}) \tag{1}$$

and

$$\psi_1(\boldsymbol{k}, \boldsymbol{r}) = \frac{1}{\sqrt{N}} \sum_{\boldsymbol{R}} e^{i\boldsymbol{k}\cdot\boldsymbol{R}}\, b_1(\boldsymbol{r} - \boldsymbol{R} - \boldsymbol{\tau}) , \tag{2}$$

where $\boldsymbol{\tau}$ is the vector joining the two atoms in the primitive cell and the subscripts on b refer to the atoms in the primitive cell. In the diamond structure crystals we take $b_0(\boldsymbol{r}) = b_1(\boldsymbol{r})$, but in the zincblende crystals the two functions are different.

In order to have

$$\langle \psi_i(\boldsymbol{k}, \boldsymbol{r}) | \psi_j(\boldsymbol{k}, \boldsymbol{r}) \rangle = \delta_{ij}; \qquad i, j = 0, 1 , \tag{3}$$

we must require that the tight-binding functions on different atomic sites be orthonormal:

$$\langle b_0(\boldsymbol{r} - \boldsymbol{R}_m) | b_1(\boldsymbol{r} - \boldsymbol{R}_n - \boldsymbol{\tau}) \rangle = 0 , \tag{4}$$

$$\langle b_i(\boldsymbol{r}) | b_i(\boldsymbol{r}) \rangle = 1 . \tag{5}$$

These conditions can always be accomplished by a method due to Löwdin [6, 9] without affecting the symmetry of the basis functions.

The basic problem of the tight-binding method is to find the matrix elements of the Hamiltonian between the various basis states. We will consider here only the case where we have only one set of s-, p_x-, p_y-, and p_z-orbitals at each atomic site. We will denote these by s_0, x_0, y_0, z_0 or s_1, x_1, y_1, z_1 where the subscripts as before refer to the atoms in the primitive cell. The Hamiltonian matrix elements between an s- and a p-state on the same atom or two different p-states on the same atom are zero because of symmetry in diamond and zincblende crystals. The matrix elements between these basis functions have been derived in reference [6]. The 8×8 secular determinant representing all possible nearest-neighbor interactions between the tight-binding s- and p-orbitals centered on each atom in the crystal is

$$
\begin{array}{c|cccccccc}
 & s_0 & s_1 & x_0 & y_0 & z_0 & x_1 & y_1 & z_1 \\
\hline
s_0 & E_{s_0}-E(\boldsymbol{k}) & V_{ss}g_0 & 0 & 0 & 0 & V_{s_0p}g_1 & V_{s_0p}g_2 & V_{s_0p}g_3 \\
s_1 & V_{ss}g_0^* & E_{s_1}-E(\boldsymbol{k}) & -V_{s_1p}g_1^* & -V_{s_1p}g_2^* & -V_{s_1p}g_3^* & 0 & 0 & 0 \\
x_0 & 0 & -V_{s_1p}g_1 & E_{p_0}-E(\boldsymbol{k}) & 0 & 0 & V_{xx}g_0 & V_{xy}g_3 & V_{xy}g_1 \\
y_0 & 0 & -V_{s_1p}g_2 & 0 & E_{p_0}-E(\boldsymbol{k}) & 0 & V_{xy}g_3 & V_{xx}g_0 & V_{xy}g_1 \\
z_0 & 0 & -V_{s_1p}g_3 & 0 & 0 & E_{p_0}-E(\boldsymbol{k}) & V_{xy}g_1 & V_{xy}g_2 & V_{xx}g_0 \\
x_1 & V_{s_0p}g_1^* & 0 & V_{xx}g_0^* & V_{xy}g_3^* & V_{xy}g_1^* & E_{p_1}-E(\boldsymbol{k}) & 0 & 0 \\
y_1 & V_{s_0p}g_2^* & 0 & V_{xy}g_3^* & V_{xx}g_0^* & V_{xy}g_2^* & 0 & E_{p_1}-E(\boldsymbol{k}) & 0 \\
z_1 & V_{s_0p}g^* & 0 & V_{xy}g_1^* & V_{xy}g_1^* & V_{xx}g_0^* & 0 & 0 & E_{p_1}-E(\boldsymbol{k})
\end{array} = 0 . \tag{6}
$$

For diamond structure crystals $E_{s_0} = E_{s_1}$, $E_{p_0} = E_{p_1}$, and $V_{s_0p} = V_{s_1p}$, and from this point we will drop the subscripts for these crystals. The functions g_0, g_1, g_2, and g_3 in (6) are given by

$$g_0(\boldsymbol{k}) = \cos\pi\frac{k_1}{2}\cos\pi\frac{k_2}{2}\cos\pi\frac{k_3}{2} - i\sin\pi\frac{k_1}{2}\sin\pi\frac{k_2}{2}\sin\pi\frac{k_3}{2}, \tag{7}$$

$$g_1(\boldsymbol{k}) = -\cos\pi\frac{k_1}{2}\sin\pi\frac{k_2}{2}\sin\pi\frac{k_3}{2} + i\sin\pi\frac{k_1}{2}\cos\pi\frac{k_2}{2}\cos\pi\frac{k_3}{2}, \tag{8}$$

$$g_2(\boldsymbol{k}) = -\sin\pi\frac{k_1}{2}\cos\pi\frac{k_2}{2}\sin\pi\frac{k_3}{2} + i\cos\pi\frac{k_1}{2}\sin\pi\frac{k_2}{2}\cos\pi\frac{k_3}{2}, \tag{9}$$

$$g_3(\boldsymbol{k}) = -\sin\pi\frac{k_1}{2}\sin\pi\frac{k_2}{2}\cos\pi\frac{k_3}{2} + i\cos\pi\frac{k_1}{2}\cos\pi\frac{k_2}{2}\sin\pi\frac{k_3}{2}, \tag{10}$$

where $\boldsymbol{k} = (2\pi/a)\,(k_1, k_2, k_3)$.

For diamond structure crystals, the parameters appearing in (6) are related to those of Slater and Koster [6] by

$$\left.\begin{array}{ll} E_s = E_{s,s}\,(000)\,, & E_p = E_{x,x}\,(000)\,, \\ V_{ss} = 4E_{s,s}\,(\frac{1}{2}\,\frac{1}{2}\,\frac{1}{2})\,, & V_{xx} = 4E_{x,x}\,(\frac{1}{2}\,\frac{1}{2}\,\frac{1}{2})\,, \\ V_{xy} = 4E_{x,y}\,(\frac{1}{2}\,\frac{1}{2}\,\frac{1}{2})\,, & V_{sp} = 4V_{s,x}\,(\frac{1}{2}\,\frac{1}{2}\,\frac{1}{2})\,. \end{array}\right\} \tag{11}$$

Before describing the total interaction between s- and p-states, it is interesting to look at each one separately. If we set the s–p interaction parameters V_{s_0p} and V_{s_1p} equal to zero, the 8×8 matrix (6) decouples into a 2×2 and a 6×6 matrix. The energy eigenvalues of the 2×2 matrix, which describes the s-states, are given by

$$E(\boldsymbol{k}) = E_s \pm V_{ss}|g_0(\boldsymbol{k})| \tag{12}$$

for diamond structure crystals. Although this expression is very simple, it nevertheless provides a very good description of the lowest valence band in these crystals. Specifying the width of the band (which is about 3.5 to 4.0 eV in Si and Ge) determines the band structure to within a few tenths of an eV throughout the Brillouin zone. The largest errors (compared to calculations based on the empirical pseudopotential method (EPM)) occur along the Λ-direction and along the Z-direction which runs between the symmetry points X $= (2\pi/a)\,(1, 0, 0)$ and W $= (2\pi/a)\,(1, \frac{1}{2}, 0)$ of the Brillouin zone. Along this

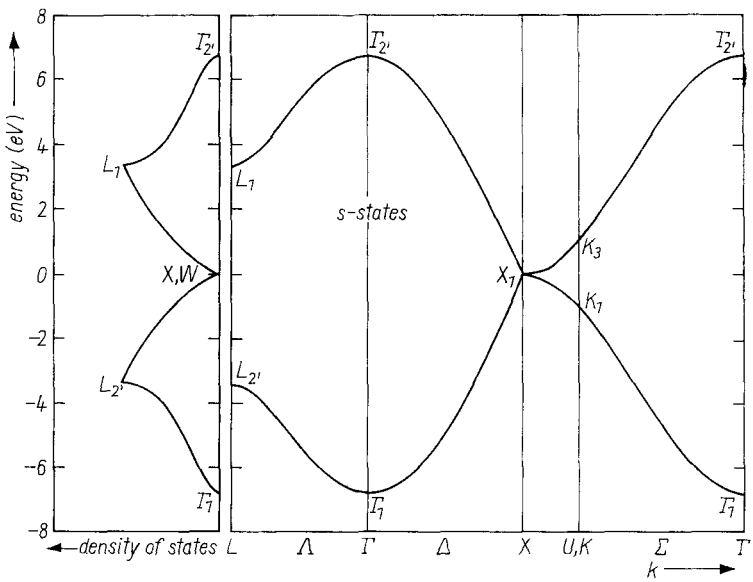

Fig. 1. Band structure and density of states of s-states for diamond structure crystals

direction the two bands are degenerate (by symmetry) and have no dispersion. The second valence band in the group IV crystals is p-like at Γ and (12) does not therefore provide a valid description for this band. The band structure and density of states associated with the tight-binding s-like bands is shown in Fig. 1. The dip in the density of states occurs near the line X → W in the Brillouin zone. For $V_{ss} < 0$ the lower-energy band is bonding at Γ and the higher band is antibonding. For $V_{ss} > 0$ the order of the bonding–antibonding states is reversed. For the zincblende crystals the analog of (12) is

$$E(\boldsymbol{k}) = \frac{E_{s_0} + E_{s_1}}{2} \pm \sqrt{\left(\frac{E_{s_0} - E_{s_1}}{2}\right)^2 + |V_{ss} g_0(\boldsymbol{k})|^2}\,, \tag{13}$$

whereas as a result of inversion symmetry the two bands were degenerate at X in the diamond structure crystals and a gap of magnitude $|E_{s_0} - E_{s_1}|$ opens up at X for the zincblende crystals. The maximum of the first band and the minimum of the second one still occur at X. But unlike the case of the group IV crystals the bands approach X with zero slope, and this results in a sharp peak in the density of states (not shown) for states near X. Except for this structure the s-band density of states in the group IV and zincblende crystals are very similar to each other.

The band structure and density of states associated with the six p-states of the group IV crystals is shown in Fig. 2 for $V_{xx} = 0$, $V_{xy} = 6.8$, and $E_p = 0$. The sharp rise and fall of the curve near threshold occurs at $\Sigma_1^{\min}$ and is very similar to the $\Sigma_1^{\min}$ edge observed in the density of states of a number of diamond and zincblende crystals [10 to 12]. As in the case of the s-bands there is no dispersion along the line joining the points X and W of the Brillouin zone, and the dip in the density of states corresponds to these states. The overall shape of the curves for the s- and p-states are similar in the region near the density-of-states minimum. For the zincblende crystals the band

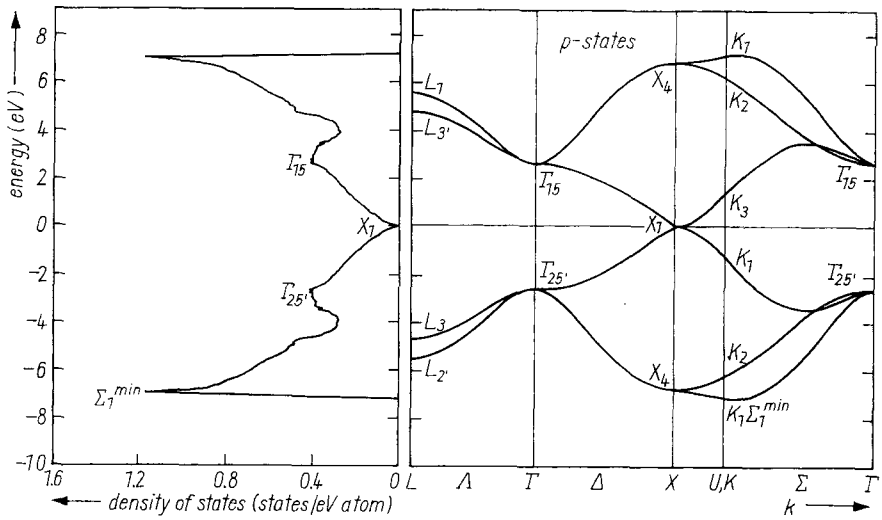

Fig. 2. Band structure and density of states of p-states for diamond structure crystals

structure and density of states for the p-states is similar to that of Fig. 2. The maximum of the lower three bands and the minimum of the upper three bands occur at X and are separated by a gap. The zero slope of the bands at X gives rise, as in the case of the s-states, to a sharp structure in the density of states (not shown). Except for this structure the densities of states of the p-bands in the group IV and the zincblende crystals are very similar as may be expected.

Sometimes it is more convenient (see, e.g., surface calculations [7]) to use tight-binding orbitals directed along the bond directions. The parameters which appear in this approach can be easily related to s–p interaction parameters. This can be done by taking the Hamiltonian matrix elements between the directed sp^3 orbitals shown in Fig. 3. The results for diamond structure crystals in Hirabayashi's [7] notation are:

$$\gamma_1 = \langle\varphi_i| H |\varphi_i\rangle = \tfrac{1}{4}(E_s + 3E_p)\,, \tag{14}$$

$$\gamma_2 = \langle\varphi_1| H |\varphi_2\rangle = \tfrac{1}{4}(E_s - E_p)\,, \tag{15}$$

$$\gamma_3 = \langle\varphi_1| H |\varphi_8\rangle = \tfrac{1}{16}(V_{ss} - 3V_{xx} - 6V_{xy} - 6V_{sp})\,, \tag{16}$$

$$\gamma_4 = \langle\varphi_2| H |\varphi_8\rangle = \tfrac{1}{16}(V_{ss} + V_{xx} + 2V_{xy} - 2V_{sp})\,, \tag{17}$$

$$\gamma_5 = \langle\varphi_2| H |\varphi_5\rangle = \tfrac{1}{16}(V_{ss} + V_{xx} - 2V_{xy} + 2V_{sp})\,, \tag{18}$$

$$\gamma_6 = \langle\varphi_2| H |\varphi_7\rangle = \tfrac{1}{16}(V_{ss} - 3V_{xx} + 2V_{xy} + 2V_{sp})\,. \tag{19}$$

The parameter γ_1 appears in the diagonal matrix elements and can be taken equal to zero. The parameters γ_2 and γ_3 are the same as the parameters V_1 and V_2 of Weaire and Thorpe [2], and from Fig. 3 it can be expected that they represent the most important interactions. The properties of a model Hamiltonian based only on these two types of interactions has been studied in detail by Weaire and Thorpe [2, 13] and has been employed in a number of calculations involving crystalline polytypes of Si and Ge [3]. These calculations show that the two-parameter model gives a relatively good description of the lower "s-like"

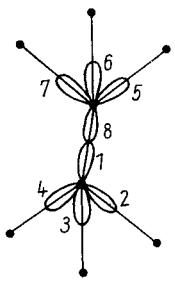

Fig. 3. Directed sp^3 orbitals on two adjacent tetrahedrons. The different possible interactions of the orbitals on the nearest-neighbor atoms are given in Section 2

valence bands, but gives a poor description of the higher p-like bands which appear as δ-functions in the density of states. The inclusion of the other interactions broadens the δ-functions and gives a better description of the valence bands.

For zincblende crystals we need three extra parameters to describe the overlaps corresponding to nearest-neighbor s–p interactions. The interaction parameters are:

$$\alpha_1 = \langle\varphi_1| H |\varphi_1\rangle = \tfrac{1}{4}(E_{s_0} + 3E_{p_0}) , \tag{20}$$

$$\beta_1 = \langle\varphi_8| H |\varphi_8\rangle = \tfrac{1}{4}(E_{s_1} + 3E_{p_1}) , \tag{21}$$

$$\alpha_2 = \langle\varphi_1| H |\varphi_2\rangle = \tfrac{1}{4}(E_{s_0} - E_{p_0}) , \tag{22}$$

$$\beta_2 = \langle\varphi_7| H |\varphi_8\rangle = \tfrac{1}{4}(E_{s_1} - E_{p_1}) , \tag{23}$$

$$\alpha_3 = \beta_3 = \langle\varphi_1| H |\varphi_8\rangle = \tfrac{1}{16}(V_{ss} - 3V_{xx} - 6V_{xy} - 3V_{s_0p} - 3V_{s_1p}) , \tag{24}$$

$$\alpha_4 = \langle\varphi_2| H |\varphi_8\rangle = \tfrac{1}{16}(V_{ss} + V_{xx} + 2V_{xy} - 3V_{s_0p} + V_{s_1p}) , \tag{25}$$

$$\beta_4 = \langle\varphi_1| H |\varphi_5\rangle = \tfrac{1}{16}(V_{ss} + V_{xx} + 2V_{xy} + V_{s_0p} - 3V_{s_1p}) , \tag{26}$$

$$\alpha_5 = \langle\varphi_2| H |\varphi_5\rangle = \tfrac{1}{16}(V_{ss} + V_{xx} - 2V_{xy} + V_{s_0p} + V_{s_1p}) , \tag{27}$$

$$\alpha_6 = \langle\varphi_2| H |\varphi_7\rangle = \tfrac{1}{16}(V_{ss} - 3V_{xx} + 2V_{xy} + V_{s_0p} + V_{s_1p}) . \tag{28}$$

The fact that the interactions represented by α_4 and β_4 are different is caused by the lack of inversion symmetry.

It can be shown that independent of the choice of the interaction parameters $\gamma_1, \ldots, \gamma_6$ (diamond structures) and $\alpha_1, \ldots, \alpha_6$, $\beta_1, \ldots, \beta_4$ (zincblendes), the bands have no dispersion along the symmetry direction Z which goes through the points $X = (2\pi/a)(1, 0, 0)$ and $W = (2\pi/a)(1, \frac{1}{2}, 0)$ of the Brillouin zone. Other calculations such as those based on the empirical pseudopotential method (EPM) show [10], however, a dispersion of ≈ 1 eV between X and W for the upper two valence bands. This dispersion is reflected in the density of states where each of these points gives rise to a characteristic and well resolved peak. To obtain this result in the tight-binding calculation it is necessary to include at least one second-nearest-neighbor interaction. Fig. 4 shows the density of states of a crystal such as Ge with and without second-nearest-neighbor interactions. For the nearest-neighbor calculation the parameters used were (in eV): $(E_p - E_s) = 8.41$, $V_{ss} = -6.78$, $V_{xx} = 2.62$, $V_{xy} = 6.82$, and $V_{sp} = 5.31$. The second-nearest-neighbor interaction we have used (in Fig. 4) arises from the overlap of a p_x-orbital at the origin with a p_x-orbital separated by a lattice vector of the type $(0, \pm\frac{1}{2}, \pm\frac{1}{2})\,a$. Its effect is to change the diagonal matrix

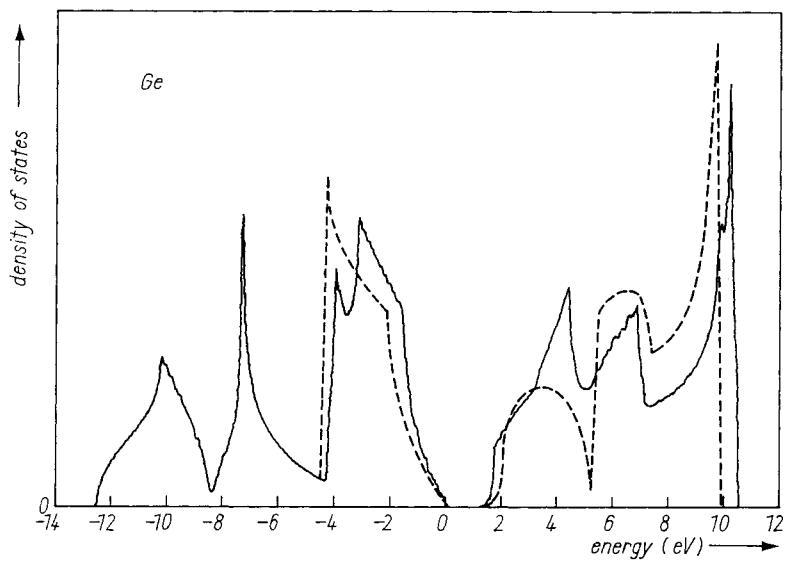

Fig. 4. The density of states (in arbitrary anits) of Ge with an without second-nearest-neighbor interaction. The second-nearest-neighbor interaction splits the energies at X and W and gives rise to extra structure in the density of states. – – – Nearest-neighbor interaction, ——— one second-nearest-neighbor interaction

elements to $\langle x_i | H | x_i \rangle \to E_p + U_{xx} \cos k_2 \cos k_3$, etc. for diamond structure crystals. The interaction U_{xx} is denoted by $4E_{xx}(011)$ in [6]. The interaction parameters when both nearest- and second-nearest interactions were used (Fig. 4) are: $(E_p - E_s) = 8.41$, $V_{ss} = -6.78$, $V_{xx} = 1.62$, $V_{xy} = 6.82$, $V_{sp} = 5.31$, and $U_{xx} = -1.0$ (eV). The resulting density of states in Fig. 4 shows the separate structures arising from the points X and W. These structures coalesce into a single peak when U_{xx} is set equal to zero. It should be pointed out here that not all second-nearest-neighbor interactions are useful in broadening the bands along Z. Interactions between two s-states or between s- and p-states separated by a primitive lattice vector have no effect on the dispersion along Z which is affected mainly by second-nearest-neighbor interactions between p-states, the largest [6] one being U_{xx}.

3. Results for C, Ge, Si, GaAs, and ZnSe

Since there is not sufficient information on the valence bands of C, we have used only nearest-neighbor interactions in our calculations on C. The parameters were obtained by fitting to the results of a variational calculation [14], and they are shown in Table 1. The energy eigenvalues are compared to other calculations in Table 2 and the resulting band structures and densities of states are shown in Fig. 5. Table 2 shows good agreement between the simple tight-binding calculation and the variational calculations [14] for the valence bands of C. The results are also very similar to those obtained from an APW [15][2]) calculation. The conduction bands are not well reproduced by the simple tight-binding method except at Γ where the splittings were fitted.

[2]) This paper gives many references to earlier theoretical and experimental work on C.

Table 1

Tight-binding interaction parameters (in eV) for C, Si, and Ge. The parameter U_{xx} represents a second-nearest-neighbor interaction. The parameter E_s determines the zero of energy and is arbitrary

	E_s	$(E_p - E_s)$	V_{ss}	V_{sp}	V_{xx}	V_{xy}	U_{xx}
C	—	7.40	−15.2	10.25	3.0	8.30	—
Si	—	7.20	− 8.13	5.88	1.71	7.51	−1.46
Ge	—	8.41	− 6.78	5.31	1.62	6.82	−1.0

Table 2

Comparison of the energy eigenvalues of C, Si, and Ge at some symmetry points in the Brillouin zone. The energies in (eV) are measured relative to the top of the valence bands at $\Gamma_{25'}$

state	C		Si		Ge	
	tight--binding	DVM [14]	tight-binding	EPM [16]	tight-binding	EPM [17]
$\Gamma_{25'}$	0	0	0	0	0	0
Γ_1	−19.6	−19.6	−12.16	−12.16	−12.57	−12.57
Γ_{15}	6.0	6.0	3.42	3.42	3.24	3.24
$\Gamma_{2'}$	10.8	10.8	4.10	4.10	0.99	0.99
$L_{2'}$	−15.2	−14.5	−9.44	9.57	−10.30	−10.30
L_1	−9.8	−11.7	−7.11	−6.98	−7.52	−7.42
$L_{3'}$	−2.6	−2.4	−1.44	−1.23	−1.60	−1.44
X_1	−11.6	−11.6	−7.70	−7.70	−8.60	−8.56
X_4	−5.3	−5.3	−2.87	−2.87	−3.30	−3.20
$\Sigma(0.5, 0.5, 0)$	−2.35	—	−3.84	−3.74	−3.80	−3.80
$\Sigma(0.7, 0.7, 0)$	−1.83	—	−4.32	−4.46	−4.29	−4.29

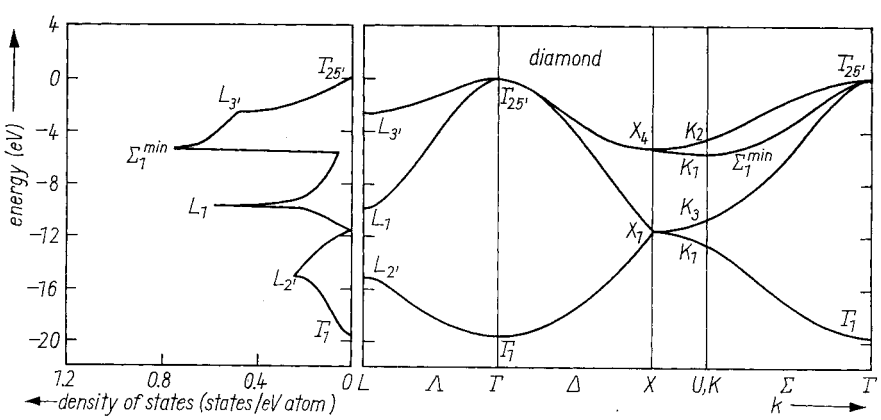

Fig. 5. Band structure and density of states of diamond

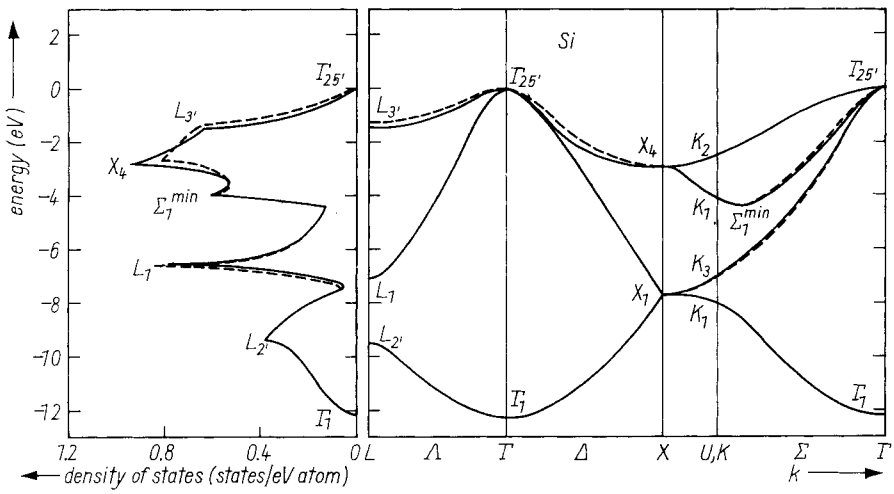

Fig. 6. Tight-binding band structure and density of states of Si as compared to the results obtained from empirical pseudopotential calculations [16]. ——— Tight binding, — — — EPM

For Si and Ge we have used one second-nearest-neighbor interaction in addition to the nearest-neighbor interactions in the calculations. The nature of these interactions was discussed in Section 2. The interaction parameters for Si and Ge are listed in Table 1 and the eigenvalues at some symmetry points in the Brillouin zone are compared to the EPM values (for Si see [16], for Ge [17]) in Table 2. The corresponding band structures and densities of states are shown in Fig. 6 and 7 and compared to those obtained from recent EPM calculations [16, 17] involving non-local (angular-momentum-dependent) potentials. The agreement in all cases is within a few tenths of an eV for the valence bands, but for the conduction bands the method is not as successful. For the sake of completeness we give in Tables 3 and 4 the interaction parameters for C, Si, and

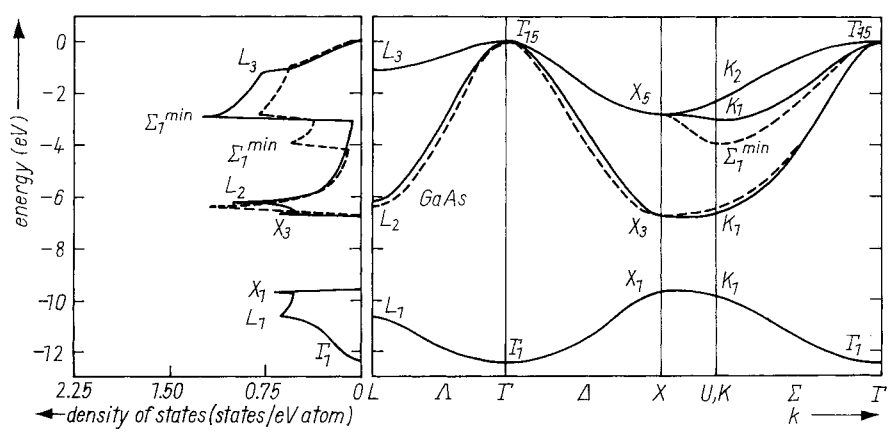

Fig. 7. Tight-binding band structure and density of states of Ge as compared to the results obtained from empirical pseudopotential calulations. [17]. ——— Tight binding. — — — EPM

Table 3

Interaction parameters (in eV) appropriate for C, Si, and Ge when second-nearest-neighbor interactions are ignored. The parameter E_s is arbitrary

	E_s	$(E_p - E_s)$	V_{ss}	V_{sp}	V_{xx}	V_{xy}
C	—	7.40	−15.2	10.25	3.0	8.3
Si	—	7.20	−8.13	5.88	3.17	7.51
Ge	—	8.41	−6.78	5.31	2.62	6.82

Table 4

Interaction parameters (in eV) between directed orbitals for C, Si, and Ge. These parameters are related to those in Table 3 through the equations given in Section 2. The parameter γ_1 can be chosen arbitrarily

	γ_1	γ_1	γ_2	γ_3	γ_5	γ_6
C	—	−1.85	−8.47	−1.01	−0.52	0.81
Si	—	−1.80	−6.13	−0.11	−0.51	0.57
Ge	—	−2.10	−5.46	−0.07	−0.45	0.60

Ge if only nearest-neighbor interactions are used. These tables show that the strength of nearly every interatomic interaction decreases as we go from C to Si to Ge.

Dresselhaus and Dresselhaus [5] have used a tight-binding Hamiltonian, related to that of Slater and Koster [6] by a unitary transformation, to make a detailed study of the valence and conduction bands in Si and Ge. Twelve first- and second-nearest-neighbor interactions were used to fit the main optical gaps and effective masses. The magnitude of the second-nearest-neighbor interactions are small compared to the first-nearest-neighbor interactions which are consistent with the values we have obtained by fitting the valence bands of

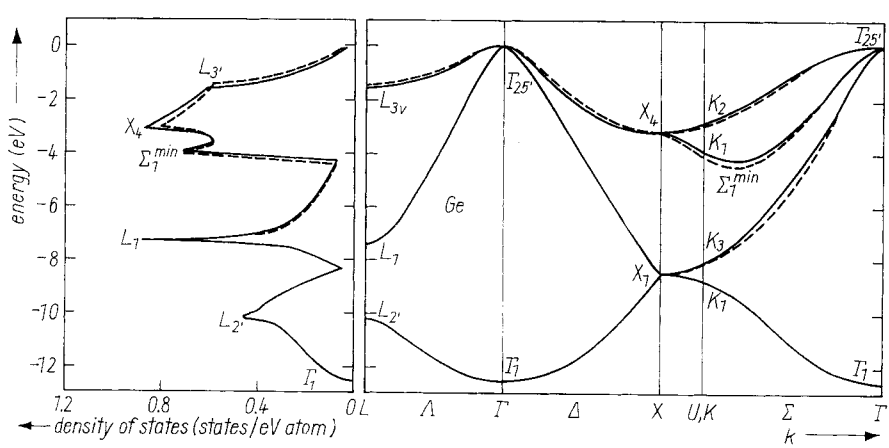

Fig. 8. Tight-binding band structure and density of states of GaAs compared to the results of EPM calculations [18]. ——— Tight binding, – – – EPM. (Read $L_{3'v}$ instead of L_{3v})

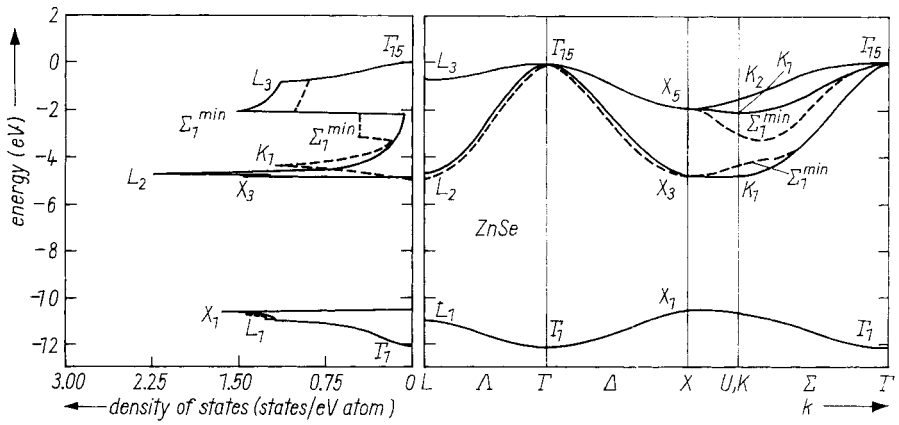

Fig. 9. Tight-binding band structure and density of states of ZnSe compared to the results of EPM calculations [19]. ——— Tight binding, — — — EPM

Si and Ge. We find that in order to obtain more accurate conduction bands we need to use more second-nearest-neighbor interactions, but as our results show, a few parameters are sufficient to give an accurate description of the valence bands and an approximate description of the first few conduction bands.

In the case of the zincblende crystals GaAs and ZnSe we have only used nearest-neighbor interactions for convenience. A second-nearest-neighbor interaction between the Ga or Zn p-states, similar to the one used for Si and Ge, is, however, necessary to broaden the upper two valence bands. The band structures and densities of states for GaAs and ZnSe are shown in Fig. 8 and 9 and compared to non-local (angular-momentum-dependent) EPM calculations [18, 19]. The interaction parameters are listed in Tables 5 and 6. The largest error

Table 5

Interaction parameters (in eV) for GaAs and ZnSe. The four intra-atomic parameters E_{s_0}, E_{s_1}, E_{p_0}, and E_{p_1} give information only on the relative energy differences between the tight-binding s- and p-functions. The subscripts 0 and 1 refer to As (or Se) and Ga (or Zn), respectively

	E_{s_0}	E_{s_1}	E_{p_0}	E_{p_1}	V_{ss}	V_{s_0p}	V_{s_1p}	V_{xx}	V_{xy}
GaAs	−6.01	−4.79	0.19	4.59	−7.00	7.28	3.70	0.93	4.72
ZnSe	−8.92	−0.28	0.12	7.42	−6.14	5.47	4.73	0.96	4.38

in the band structures occur for the states denoted by $\Sigma_1^{\min}$. The tight-binding results are actually much closer to older EPM calculations which used local pseudopotentials resulting in upper valence bands which are narrower. Ultraviolet and X-ray photoemission spectra, however, reveal a larger width for these bands than those indicated by local pseudopotentials, and this has been one reason for the use of non-local pseudopotentials. The energy eigenvalues at some symmetry points in the Brillouin zone are given in Table 7 and compared to the EPM values. For more accurate conduction bands second-nearest-neighbor interactions, especially those between s- and p-states, need to be included.

Table 6

Tight-binding parameters (in eV) between directed orbitals for GaAs and ZnSe. These parameters are related to those in Table 5 through the relations given in Section 2

	α_1	β_1	α_2	β_2	$\alpha_3 = \beta_3$	α_4	β_4	α_5	α_6
GaAs	−1.36	2.25	−1.55	−2.35	−4.44	−0.92	−0.03	−0.28	0.66
ZnSe	−2.14	5.57	−2.26	−1.93	−4.12	−0.51	−0.32	−0.23	0.62

The tight-binding method allows a simple calculation of the s- and p-character of the valence bands and it is interesting to see how close to ideal sp^3 they are. We have therefore computed the average s- and p-components of the wave functions for the valence bands. We find the top two valence bands to be completely p-like in character in all five crystals. The differences in the s- and p-characters occur mainly for the first two valence bands and these are shown in Table 8. The average of the s- and p-electrons in the four valence bands of C, Si, and Ge are, C: 1.25 s, 2.75 p; Si: 1.4 s, 2.6 p; Ge: 1.5 s, 2.5 p. The ratio of the number of s- to p-electrons is 0.45 for C, 0.54 for Si, and 0.6 for Ge. Carbon is therefore as expected the closest to the ideal ratio of 0.333. In GaAs and ZnSe the first valence band is s-like around As and Se. The second valence band is mainly s-like around Ga and Zn, and p-like around As and Se.

In the simple model of Weaire and Thorpe [2] in which only two interaction parameters (equivalent to γ_2 and γ_3) are used, the bonding and antibonding p-states give rise to two δ-functions, each of weight two, in the density of states. The δ-functions correspond to doubly degenerate bands which are flat throughout the Brillouin zone. The addition of extra interactions obviously broadens these bands and the δ-functions. It is interesting to see which interactions are

Table 7

Comparison of the energy eigenvalues of GaAs and ZnSe at some symmetry points in the Brillouin zone. The energies in (eV) are measured relative to the top of the valence bands at Γ_{15}

state	GaAs		ZnSe	
	tight-binding	EPM [18]	tight-binding	EPM [19]
Γ_{15v}	0	0	0	0
Γ_{1v}	−12.4	−12.4	−12.1	−12.1
Γ_{1c}	1.6	1.6	2.9	2.9
Γ_{15c}	4.8	4.8	7.5	7.5
L_{1v}	−10.7	−10.5	−11.0	−10.9
L_{2v}	−6.2	−6.7	−4.7	−4.9
L_{3v}	−1.2	−1.2	−0.75	−0.75
L_{1c}	1.7	1.6	3.9	4.1
L_{3c}	6.0	4.8	8.3	7.9
X_{1v}	−9.7	−9.7	−10.6	−10.6
X_{3v}	−6.8	−6.8	−4.8	−4.8
X_{5v}	−2.8	−2.8	−1.9	−1.9
X_{1c}	2.2	2.2	4.7	4.7
$\Sigma_1^{\min}$	−3.1	−4.1	−2.1	−3.2

Table 8
The average s- and p-characters for the valence bands of C, Si, Ge, GaAs, and ZnSe

	band 1 s, p	band 2 s, p	bands 3, 4 s, p
C	0.84, 0.16	0.39, 0.61	≈0, 1
Si	0.9, 0.1	0.45, 0.55	≈0, 1
Ge	0.9, 0.1	0.57, 0.43	≈0, 1
GaAs	0.88, 0.12	0.61, 0.39	≈0, 1
ZnSe	0.94, 0.06	0.42, 0.58	≈0, 1

most important in producing this broadening of the bands. In the s–p interaction picture, it can be shown that if we set $V_{xx} = V_{xy}$ then we immediately obtain, for both diamond and zincblende crystals, two sets of bands which are doubly degenerate and flat throughout the Brillouin zone, independent of the magnitude of the other nearest-neighbor interactions. In the directed-orbital representation equations (18), (19) and (27), (28) show that $V_{xx} = V_{xy}$ corresponds to $\gamma_5 = \gamma_6$ (diamond structures) or $\alpha_5 = \alpha_6$ (zincblendes). Therefore, independent of the other interactions between the orbitals, if $\gamma_5 = \gamma_6$ or $\alpha_5 = \alpha_6$ we will have flat p-bands in the entire Brillouin zone. The broadening of the p-bands can be expected to be related to $V_{xx} - V_{xy}$. In fact, if we take second-nearest-neighbor interactions to be zero, then in diamond structure crystals the width of the doubly degenerate valence bands is exactly equal to $|V_{xx} - V_{xy}|$ or $4|\gamma_5 - \gamma_6|$ with the top of the bands at Γ and the bottom at X. It is obviously not a good approximation to take $V_{xx} = V_{xy}$ or $\gamma_5 = \gamma_6$. In fact we expect the interaction V_{xy} to be stronger than V_{xx} because the overlap between the orbitals x_0, y_1 is larger than the overlap between the orbitals x_0 and x_1. This is born out in Tables 1, 3, and 5.

In order to calculate the interaction parameters we used the dependence of the energy gaps (at a few points in the Brillouin zone) on the potentials. Along some symmetry directions and at some symmetry points the dependence of the energies on the potentials can be obtained in closed form. Here we list some of these relations, a number of which were first obtained in [6].

For the diamond structure crystals we have:

$$\begin{aligned} E(\Gamma_1) &= E_s + V_{ss}\,, \\ E(\Gamma_{2'}) &= E_s - V_{ss}\,, \\ E(\Gamma_{25'}) &= E_s + (E_p - E_s) + U_{xx} - V_{xx}\,, \\ E(\Gamma_{15}) &= E_s + (E_p - E_s) + U_{xx} + V_{xx}\,. \end{aligned}$$

At L the doubly degenerate eigenvalues are given by

$$E(\mathrm{L}_{3'}) = E_s + (E_p - E_s) \pm \tfrac{1}{2}(V_{xx} + V_{xy})$$

and the four non-degenerate states are

$$E(\mathrm{L}) = E_s + \left[\frac{E_p - E_s}{2}\right] \pm \frac{1}{4}(V_{ss} - V_{xx} + 2V_{xy}) \pm$$

$$\pm \frac{1}{2}\sqrt{\left[\frac{V_{ss} + V_{xx} - 2V_{xy}}{2} \mp (E_p - E_s)\right]^2 + 12\,V_{sp}^2}\,.$$

(There is a misprint in [6] for this expression, i.e., V_{ss} outside the square root is replaced by V_{sp}.) At X the energies of the doubly degenerate roots are given by:

$$E(\mathrm{X}_4) = E_s + (E_p - E_s) - U_{xx} \pm V_{xy} ,$$

$$E(\mathrm{X}_1) = E_s + \frac{E_p - E_s + U_{xx}}{2} \pm \frac{1}{2}\sqrt{(E_p - E_s + U_{xx})^2 + (2V_{sp})^2} .$$

When U_{xx} is set equal to zero, the energy of the bands for $\boldsymbol{k} = (2\pi/a)\,(1, k, 0)$ are equal to the energies at X. Along the symmetry direction $\boldsymbol{\Lambda} = (2\pi/a)\,(k,k,k)$ only the energy of the doubly degenerate bands can be obtained in closed form:

$$E(\Lambda) = E_p + U_{xx}\cos^2 \pi k \pm |V_{xx}g_0 - V_{xy}g_1| =$$

$$= E_p + U_{xx}\cos^2 \pi k \pm$$

$$\pm\sqrt{\left(V_{xx}\cos\pi^3\frac{k}{2} + V_{xy}\sin^2\pi\frac{k}{2}\cos\pi\frac{k}{2}\right)^2 + \left(V_{xx}\sin^3\pi\frac{k}{2} + V_{xp}\cos^2\pi\frac{k}{2}\sin\pi\frac{k}{2}\right)^2} .$$

Along the symmetry direction $\Delta = (2\pi/a)\,(k, 0, 0)$, the singly degenerate eigenvalues are given by

$$E(k) = E_s + \frac{E_p - E_s + U_{xx} \pm (V_{ss} + V_{xx})\cos\pi\frac{k}{2}}{2} \pm$$

$$\pm \frac{1}{2}\sqrt{\left(E_p - E_s + U_{xx} \pm (V_{ss} - V_{xx})\cos\pi\frac{k}{2}\right)^2 + \left(2V_{sp}\sin\pi\frac{k}{2}\right)^2} .$$

The doubly degenerate eigenvalues along Δ are given by

$$E = E_s + (E_p - E_s) + U_{xx}\cos\pi k \pm \sqrt{\left(V_{xx}\cos\pi\frac{k}{2}\right)^2 + \left(V_{xy}\sin\pi\frac{k}{2}\right)^2} .$$

Along the symmetry direction $\Sigma = (2/a)\,(k, k, 0)$, the energy of the fourth valence band is given by

$$E(k) = E_s + (E_p - E_s) + U_{xx}\cos\pi k - (V_{xx}\cos^2\pi k + V_{xy}\sin^2\pi k) .$$

Changing the signs of V_{xx} and V_{xy} gives the results for one of the conduction bands.

For the zincblende crystals the eigenvalues at the symmetry points Γ, X, and L are given by:

$$E(\Gamma_1) = \frac{E_{s_0} + E_{s_1}}{2} \pm \sqrt{\left(\frac{E_{s_0} - E_{s_1}}{2}\right)^2 + V_{ss}^2} ,$$

$$E(\Gamma_{15}) = \frac{E_{p_0} + E_{p_1}}{2} \pm \sqrt{\left(\frac{E_{p_0} - E_{p_1}}{2}\right)^2 + V_{xx}^2} \quad \text{(triply degenerate)} ,$$

$$E(\mathrm{X}_1) = \frac{E_{s_0} + E_{p_1}}{2} \pm \sqrt{\left(\frac{E_{s_0} - E_{p_1}}{2}\right)^2 + V_{s_0p}^2} ,$$

$$E(\mathrm{X}_3) = \frac{E_{s_1} + E_{p_0}}{2} \pm \sqrt{\left(\frac{E_{s_1} - E_{p_0}}{2}\right)^2 + V_{s_1p}^2} ,$$

$$E(\mathrm{X}_5) = \frac{E_{p_0} + E_{p_1}}{2} \pm \sqrt{\left(\frac{E_{p_0} - E_{p_1}}{2}\right)^2 + V_{xy}^2}\,,$$

$$E(\mathrm{L}_3) = \frac{E_{p_0} + E_{p_1}}{2} \pm \frac{1}{2}\sqrt{\left(\frac{E_{p_0} - E_{p_1}}{2}\right)^2 + (V_{xx} + V_{xy})^2}\,.$$

The energies of the bands for $\boldsymbol{k} = (2\pi/a)\,(1, k, 0)$ is equal to the energies at X when only the nearest-neighbor interactions listed above are used.

Acknowledgements

We would like to thank Dr. J. D. Joannopoulos for a critical reading of the paper. One of us (D. J. C.) would also like to thank J. R. Chelikowsky for supplying information on the pseudopotential calculations.

References

[1] G. G. Hall, Phil. Mag. **43**, 338 (1952); **3**, 429 (1958).
[2] D. Weaire and M. F. Thorpe, Phys. Rev. B **4**, 2508 (1971).
M. F. Thorpe, D. Weaire, and R. Alben, Phys. Rev. B **7**, 3777 (1973).
[3] J. D. Joannopoulos and M. L. Cohen, Phys. Rev. B **7**, 2644 (1973).
J. D. Joannopoulos, Ph.D. Thesis, Univ. California, 1974 (unpublished).
[4] W. A. Harrison, Phys. Rev. B **8**, 4487 (1973).
N. J. Shevchik, J. Tejeda, and M. Cardona, Phys. Rev. B **9**, 2627 (1974).
W. A. Harrison and S. Ciraci, Phys. Rev. B **10**, 1516 (1974).
[5] G. Dresselhaus and M. S. Dresselhaus, Phys. Rev. **160**, 649 (1967).
[6] J. C. Slater and G. F. Koster, Phys. Rev. **94**, 1498 (1954).
[7] K. Hirabayashi, J. Phys. Soc. Japan **27**, 1475 (1969).
[8] G. Leman and J. Friedel, J. appl. Phys. **33**, 281 (1962).
[9] P. O. Löwdin, J. chem. Phys. **18**, 365 (1950).
[10] J. R. Chelikowsky, D. J. Chadi, and M. L. Cohen, Phys. Rev. B **8**, 2786 (1973).
[11] D. E. Eastman, W. D. Grobman, J. L. Freeouf, and M. Erbudak, Phys. Rev. B **9**, 3473 (1974).
[12] L. Ley, R. A. Pollak, F. R. McFeely, S. R. Kowalczyk, and D. A. Shirley, Phys. Rev. B **9**, 600 (1974).
[13] M. F. Thorpe and D. Weaire, Phys. Rev. B **4**, 3518 (1971).
[14] G. S. Painter, D. E. Ellis, and A. R. Lubinsky, Phys. Rev. B **4**, 3610 (1971).
[15] R. Keown, Phys. Rev. **150**, 568 (1966).
[16] J. R. Chelikowsky and M. L. Cohen, to be published.
[17] J. R. Chelikowsky and M. L. Cohen, Phys. Rev. Letters **31**, 1582 (1973).
[18] J. R. Chelikowsky and M. L. Cohen, Phys. Rev. Letters **32**, 674 (1974).
[19] J. R. Chelikowsky and M. L. Cohen, Phys. Letters A **47**, 7 (1974).

(Received August 12, 1974)